JOURNAL OF MATERIALS SCIENCE 18 (1983) 2555–2562

Transformation behaviour of laser processed Fe–5% Cr, Fe–5% Ni and Fe–6% Cr–2% Ni alloys

P. A. MOLIAN*, W. E. WOOD
Department of Materials Science, Oregon Graduate Center, Beaverton, Oregon 97006, USA

The effects of rapid cooling, of the order of $10^{4\circ}$ C sec^{-1}, achieved through the laser surface alloying process, on the transformation behaviour of Fe–5% Cr, Fe–5% Ni and Fe–6% Cr–2% Ni alloys have been investigated. The solidification structures and microstructures were characterized by optical and transmission electron microscopy. The significant findings are that Fe–5% Cr alloy undergoes a massive transformation to ferrite while Fe–5% Ni and Fe–6% Cr–2% Ni alloys undergo a transformation to a structure consisting of both ferrite and martensite. The substructures of ferrite and martensite were observed to contain essentially dislocations. These alloys also exhibited two carbide precipitations namely epsilon carbide and cementite. Solidification studies revealed that cellular solidification structures were present in 5% Ni and 6% Cr–2% Ni alloys with a cell spacing of 3 μm but no solidification structures were observed in 5% Cr alloy. The influence of nature of solute and cooling rate on solidification behaviour, transformation mode and morphology of structures have been discussed.

1. Introduction

Gilbert and Owen [1] introduced the massive transformations in rapidly quenched binary alloys of iron with chromium, nickel and silicon which stimulated the phase transformation studies in these systems in terms of morphology, transformation mode and thermodynamics of transformations [2–10]. However, the factors which control the structures obtained by rapid quenching have not been completely elucidated and consistent. Several investigations on the transformations of Fe–Cr and Fe–Ni alloy systems [1–4, 8–10] resulted in disagreement over many important aspects particularly on the effect of high quench rates on the transformation of austenite to martensite. In addition to kinetics of austenite to ferrite or martensite transformation, the morphology of transformation structures received little attention and very few thin foil electron microscopic observations have been reported [3, 4, 8, 11]. In contrast to solid state transformation studies, there are no reported data on rapid solidification processing of Fe–Cr, Fe–Ni and Fe–Cr–Ni alloys.

In the light of these observations, the present study was undertaken with the objective of defining the solidification and solid state transformation structures formed in Fe–5% Cr, Fe–5% Ni and Fe–6% Cr–2% Ni alloys produced through the laser surface alloying process.

2. Experimental details

High purity iron (Ferrovac E: C–0.008%, Si–0.01%, Mn–0.01%, S–0.003%, P–0.008%) received in the form of cold-rolled ingots was vacuum degassed (10^{-7} torr) at 650° C and cut to specimens of size 715 cm x 2.5 cm x 0.64 cm. Chromium and nickel were then electrodeposited on these samples using conventional electroplating methods. Coating thicknesses employed in this

*Present address: Department of Mechanical Engineering, Iowa State University, Ames, Iowa 50011, USA.

0022–2461/83 $03.00 + .12

study were 20 μm chromium thickness to produce 5% Cr alloy, 20 μm nickel thickness to produce 5% Ni alloy, and 30 μm total chromium and nickel (chromium thickness 20 μm; nickel thickness 10 μm) thickness to produce 6% Cr–2% Ni alloy. After electrodeposition the samples were again vacuum degassed (10^{-7} torr) at 205° C to remove the entrapped hydrogen in the coatings.

The electrodeposited iron specimens were mounted on a numerically controlled X–Y table and irradiated with a 1200 W power CO_2 laser beam of 10.6 μm wavelength; the beam was defocused to a spot of 0.25 mm diameter. Multiple pass melting was carried out with a scan rate of 2.94 cm sec^{-1} and an interval of 0.025 cm between passes. The average penetration depths obtained were 500 μm for chromium-alloyed iron, 520 μm for nickel-alloyed iron, and 625 μm for chromium-and-nickel-alloyed iron. The average cooling rate estimated based on heat transfer analysis [16] and solidification structures [12] to be approximately 2.0×10^4 ° C sec^{-1}.

Microstructural and compositional analysis consisted of optical, scanning and transmission electron microscopy, and energy and wavelength X-ray microprobe analysis. Extensive transmission electron microscopy was carried out to characterize and identify the transformation substructures such as dislocations, precipitates and so forth. Thin foils for transmission work were taken from mid-region of laser alloyed zone. Slices 0.6 mm thick were mechanically sectioned using flood cooling to avoid tempering. A series of 120, 240, 400 and 600 grit SiC papers were then used to reduce the thickness to 0.10 mm. Discs of 3 mm diameter were punched and thinned in a solution containing 5% perchloric acid in 2-butoxy ethanol with 80 V applied voltage at −10° C using a twin jet polisher. The foils were then examined in a Hitachi HU-11B electron microscope operated at 100 kV. For optical and scanning electron microscopy, the samples were polished and etched in 2% Nital, Villella's and mixed acid etchants.

3. Results and discussion

3.1. Fusion-zone studies

Fig. 1 shows the transverse section of laser-alloyed zone typically observed in multiple pass laser-treated samples. Studies on laser-alloyed zones revealed that the desired composition and cooling rate can be obtained by controlling the initial coating thickness and penetration depth. For the given laser beam parameters, both 20 μm chromium and nickel coating thicknesses produced an average penetration depth of 500 μm while 30 μm total chromium and nickel thickness produced a penetration depth of 625 μm. The compositions were analysed by energy and wavelength X-ray microprobe analysis and determined to be 5% Cr, 5% Ni and 6% Cr–2% Ni alloys, respectively.

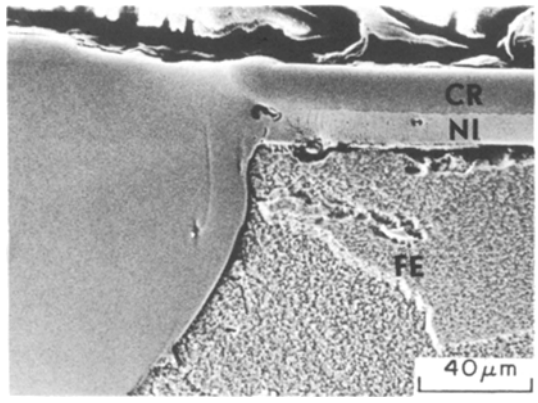

Figure 1 Transverse section of laser surface alloyed zone showing coatings and fusion zone.

3.2. Solidification behaviour

Fe–5% Cr alloy did not exhibit any solidification structure although several etchants were tried and none found to be effective. On the other hand, cellular solidification structures were readily obtained in Fe–5% Ni and Fe–6% Cr–2% Ni alloys. The average cell size and cell spacing were measured to be 3.3 and 2.9 μm for 5% Ni alloy and 3.5 and 3.1 μm for 6% Cr–2% Ni alloy, respectively. Fig. 2 illustrates these aspects of solidification structures for 5% Ni and 6% Cr–2% Ni alloys. Solidification structures are consequences of solute segregation produced by constitutional undercooling. This solute segregation is largely determined by the shape of the solidus and liquidus of the constitution diagram for the segregating components. It appears that the difference in constitution diagrams between Fe–Cr (isomorphous) and both Fe–Ni and Fe–Cr–Ni (peritectic) systems is responsible for the absence or presence of solidification structures. The presence of cellular solidification structures in 5% Ni and 6% Cr–2% Ni alloys suggest that steep temperature gradients and slow growth rates prevailed during laser surface alloying of chromium and/or nickel on iron. Cell spacing is an important structural charac-

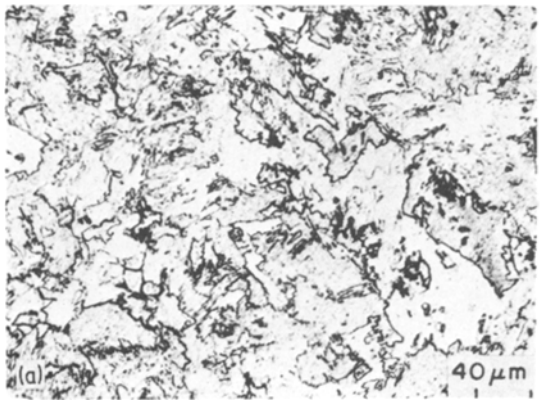

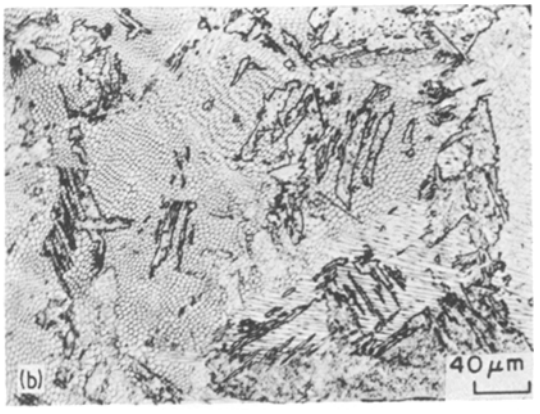

Figure 2 Light micrographs of laser-processed iron alloys: (a) Fe–5% Cr; (b) Fe–5% Ni; (c) Fe–6% Cr–2% Ni.

teristic to determine the cooling rate [12]. Using Fleming's relation [12] between cell spacing and cooling rates, the cooling rates were determined to be 1.3×10^4 °C sec^{-1} for 5% Ni alloy and 1.0×10^4 °C sec^{-1} for 6% Cr–2% Ni alloy.

3.3. Solid state transformations

3.3.1. Optical and transmission microscopy

Figs. 3a to c illustrate the optical micrographs of laser surface alloyed 5% Cr, 5% Ni and 6% Cr–2% Ni alloys. The morphological features observed in these micrographs suggest that the microstructures of 5% Cr and 5% Ni alloys to be massive ferrite and 6% Cr–2% Ni alloy to be martensitic. However, extensive transmission electron microscopy examination of these alloys revealed that 5% Cr alloy showed completely ferritic (Fig. 4) but 5% Ni and 6% Cr–2% Ni alloys exhibited a microstructure consisting of both ferrite and martensite (Figs. 5 and 6). It is interesting to note that there is a marked contrast in the transformation behaviour between 5% Cr and 5% Ni and 6% Cr–2% Ni alloys though all these alloys underwent austenitic transformation.

3.3.2. Transformations in Fe–5% Cr alloy

The morphology of ferrite grains in 5% Cr alloy as seen in optical (Fig. 3a) and in electron (Fig. 4) micrographs illustrated no apparent features that would suggest that they had arisen from shear

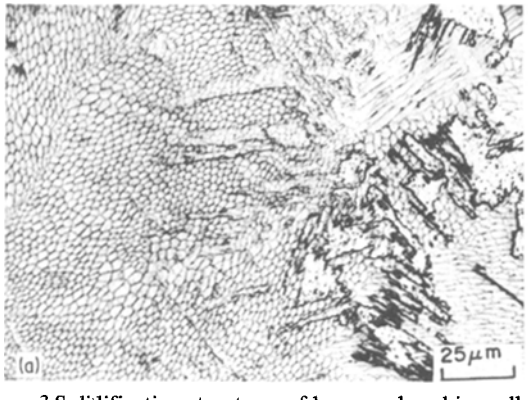

Figure 3 Solidification structures of laser-produced iron alloys: (a) Fe–5% Ni; (b) Fe–6% Cr–2% Ni.

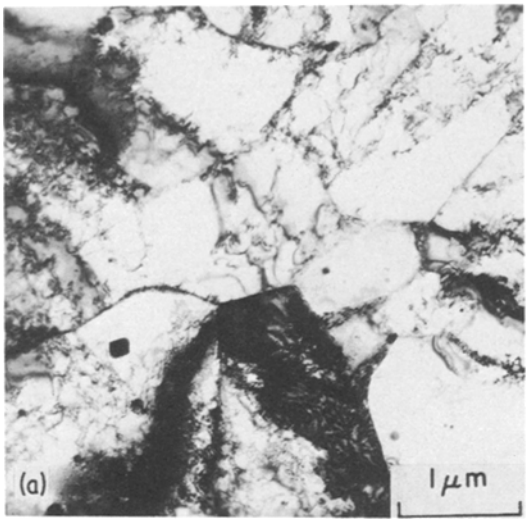

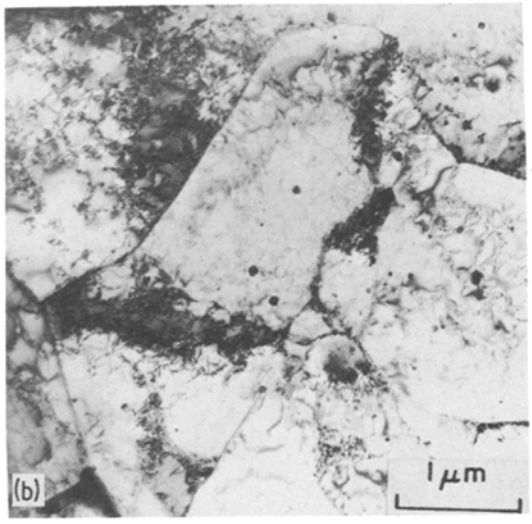

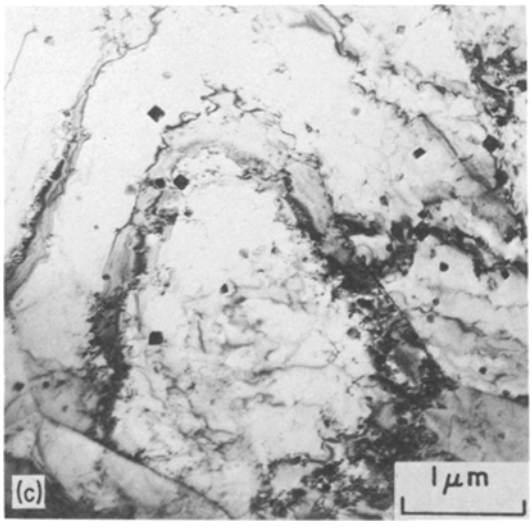

Figure 4 Transmission electron micrographs (bright-field) of laser-processed Fe–5% Cr alloy.

transformation. This type of transformation, however, could be termed as massive. Transformation by massive mechanism has been reported to occur in Fe–Cr alloys up to a quench rate of $5500^\circ C\,sec^{-1}$ by Gilbert and Owen [1]. By applying Kaufmann and Cohens' thermodynamic data on regular solution analysis, they had shown that the free energy change accompanying massive transformation is smaller that that of martensitic and concluded that rapidly quenched Fe–Cr alloys can undergo only massive transformation. Pascover and Radcliffe reported [4] equiaxed ferrite (also called "massive") in Fe–Cr alloys (0 to 10% Cr) with a quench rate of $4 \times 10^{4\,\circ} C\,sec^{-1}$. They also reported [6] that the structure of Fe–5% Cr alloy remained equiaxed ferrite by quenching at a pressure of 25 kbar. They deduced that both pressure and quenching rate were insufficient to inhibit the short-range diffusion involved in the formation of ferrite. Similar results were reported by other investigators [8, 14]. However, Wallbridge and Parr [17] had shown martensitic transformation in Fe–Cr alloys with a quench rate of $15\,000^\circ C\,sec^{-1}$ but based on a surface rumpling criterion. Bee and Honeycombe [11] also observed martensitic transformation in water-quenched specimens. In fact, Pascover and Radcliffe [4, 6] also reported martensitic transformation in Fe–Cr alloys with quench rates up to $40\,000^\circ C\,sec^{-1}$ but at a lower transformation temperature of about $500^\circ C$. Transformation temperature, i.e. the temperature at which austenite transforms to ferrite or martensite, plays an important role in deciding the type of transformation such as massive, equiaxed or martensitic. While it is well established that transformation temperature exhibited a progressive decrease with increase in cooling rate to a constant value, there is a disrepency in the values reported by several investigators of transformation temperature for a constant cooling rate [1–10]. Although transformation temperatures could not be determined in the present study, the observed characteristics of transformation behaviour suggest that the transformation temperature is higher than necessary to produce martensitic transformation. The pattern of transformation behaviour in laser-produced Fe–5% Cr alloy appears to be consistent with the

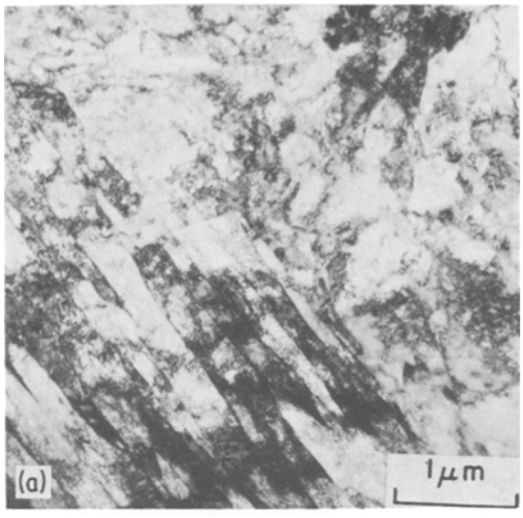

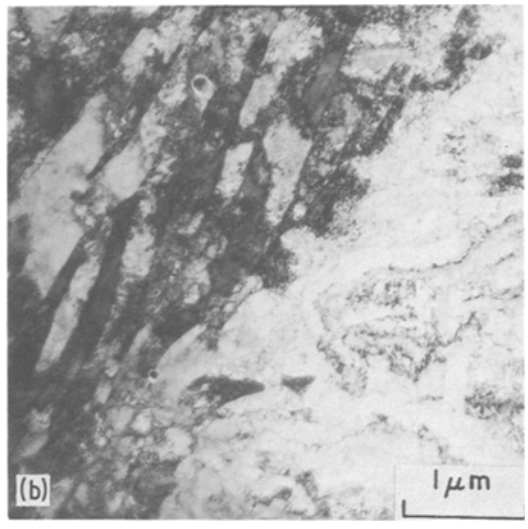

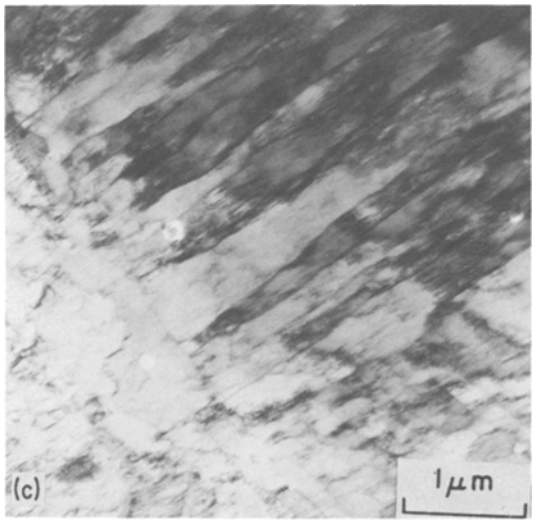

Figure 5 Transmission electron micrographs (bright-field) of laser-processed Fe–5% Ni alloy.

current understanding of the characteristic non-martensitic mode of decomposition of austenite. It is believed that a high quench rate of 10^4 ° C sec^{-1} achieved through the laser surface alloying process could not reduce the transformation temperature to a low enough level to prevent atomic mobility and permit martensitic transformation.

3.3.3. Transformations in Fe–5% Ni and Fe–6% Cr–2% Ni alloys

In contrast to the massive ferrite structures that developed in Fe–5% Cr alloy, transmission electron metallographic examination of Fe–5% Ni and Fe–6% Cr–2% Ni alloys revealed that the microstructures are composed of mixtures of massive ferrite and martensite. The Fe–Ni system is of special interest in that massive transformation was observed in alloys containing less than 15% Ni while alloys having more than 18% Ni transformed by the conventional martensitic mechanism [1, 8]. Gilbert and Owen [1] attributed the reason for obtaining martensite in alloys containing more than 18% Ni, even at a low quench rate of 5° C sec^{-1}, to the lower transformation temperature. Wilson *et al.* [9] reported massive ferrite transformation in Fe–5% Ni alloy at a quench rate of 5×10^4 ° C sec^{-1} and at a transformation temperature of 525° C. But Swanson and Parr [10] were able to surpress the massive transformation in 0 to 10% Ni alloys at a quench rate of 1.5×10^4 ° C sec^{-1} and produced martensitic structure as revealed by surface relief. They also observed that the critical cooling rate required to produce martensitic transformation is 30 000° C sec^{-1} for 1% Ni to 15 000° C sec^{-1} for 10% Ni alloy. Goodenow and Hehemann reported [8] a lath-like substructure observed in rapidly quenched (2500° C sec^{-1}) Fe–9% Ni alloy which is analogous to that of low carbon martensite. Speich and Swann [3], using thin foil microscopy, identified a lath-like cell structure with high dislocation density in alloys containing 6 to 25% Ni. But they observed the structure of alloys containing 0 to 4% Ni to be blocky grains of ferrite with low dislocation density. They attributed the discontinuous change in the transformation behaviour at 6% Ni to a change in the transformation mechanism from massive to martensitic. Unlike Fe–Cr and Fe–Ni alloy systems, there is a very limited amount of

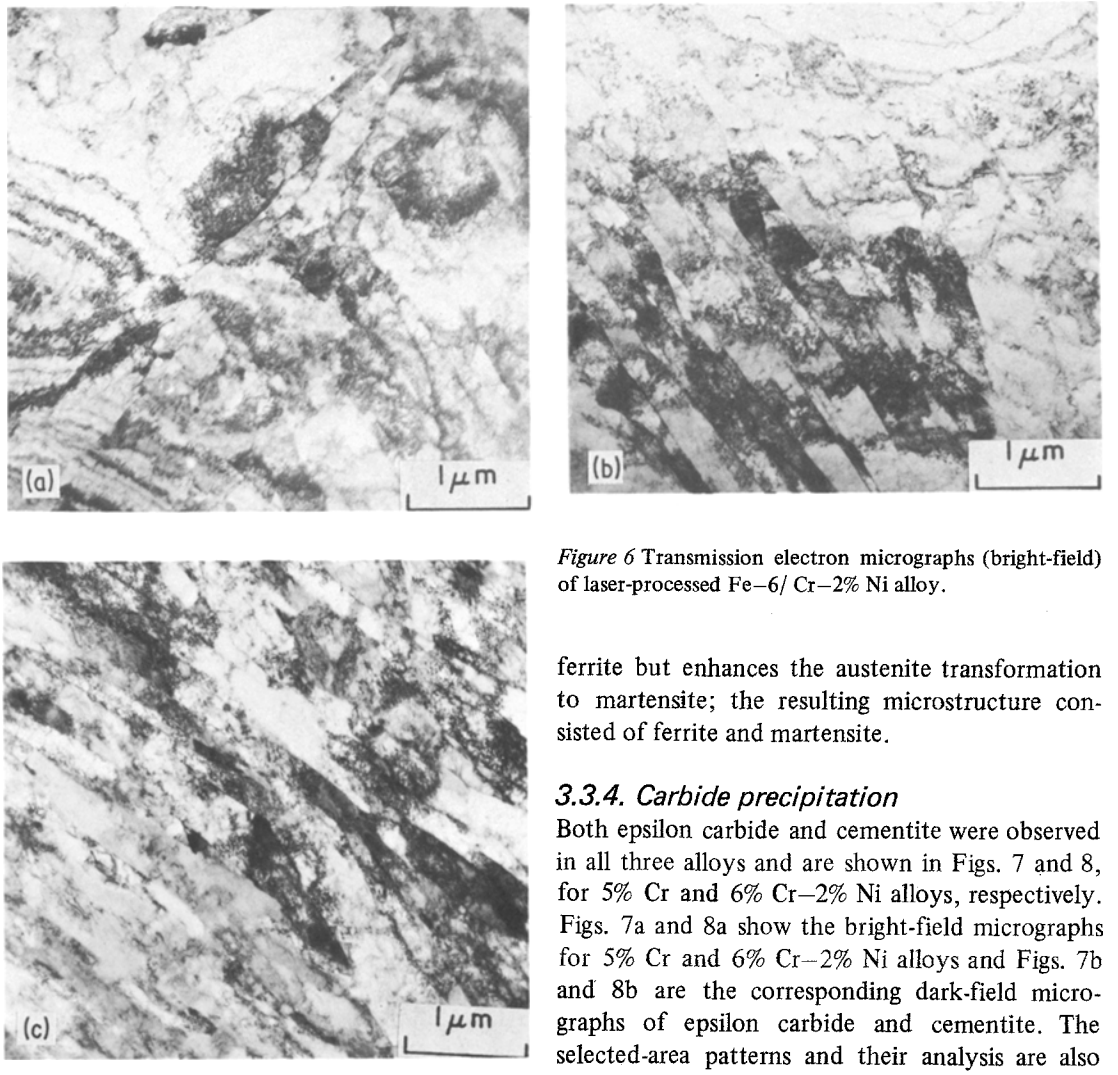

Figure 6 Transmission electron micrographs (bright-field) of laser-processed Fe–6/ Cr–2% Ni alloy.

data reported on the effect of high quench rate on the microstructures of Fe–Cr–Ni alloys. Speich [15] has plotted a non-equilibrium diagram for Fe–Cr–Ni alloy, quenched from 1100° C. According to this plot, 6% Cr–2% Ni alloy should exhibit both massive ferrite and lath martensite.

The presence of ferrite and martensite in 5% Ni and 6% Cr–2% Ni alloys suggests that there is a change in the solid state transformation mechanisms during rapid quenching. Under equilibrium conditions, as predicted by the constitution diagrams [18, 19] both the alloys undergo a transformation from austenite to ferrite through a two-phase region of ferrite and austenite. It appears that rapid quenching achieved through laser surface alloying process is able to suppress the transformation of austenite and ferrite mixture to ferrite but enhances the austenite transformation to martensite; the resulting microstructure consisted of ferrite and martensite.

3.3.4. Carbide precipitation

Both epsilon carbide and cementite were observed in all three alloys and are shown in Figs. 7 and 8, for 5% Cr and 6% Cr–2% Ni alloys, respectively. Figs. 7a and 8a show the bright-field micrographs for 5% Cr and 6% Cr–2% Ni alloys and Figs. 7b and 8b are the corresponding dark-field micrographs of epsilon carbide and cementite. The selected-area patterns and their analysis are also shown in Figs. 7 and 8. Generally, low carbon steels are not expected to contain any epsilon carbide [20] and a minimum of 0.25% C is necessary for the precipitation of epsilon carbide. This is contrary to the results of Tekin [21], who obtained epsilon carbide in as-quenched 0.1% C steels. The presence of epsilon carbide in aged low-carbon irons (C – 0.3%) was also shown by many investigators [22–25]. Wells and Butler [25] observed preferential precipitation of epsilon carbide on dislocations.

The presence of cementite and epsilon carbide is attributed either to autotempering effects or to the cyclic heat treating of laser-melted zones during multiple scanning of the laser beam in the process. It is believed that supersaturated ferrite formed during single-pass melting subsequently precipitates out carbide due to the tempering effects induced by multiple scanning.

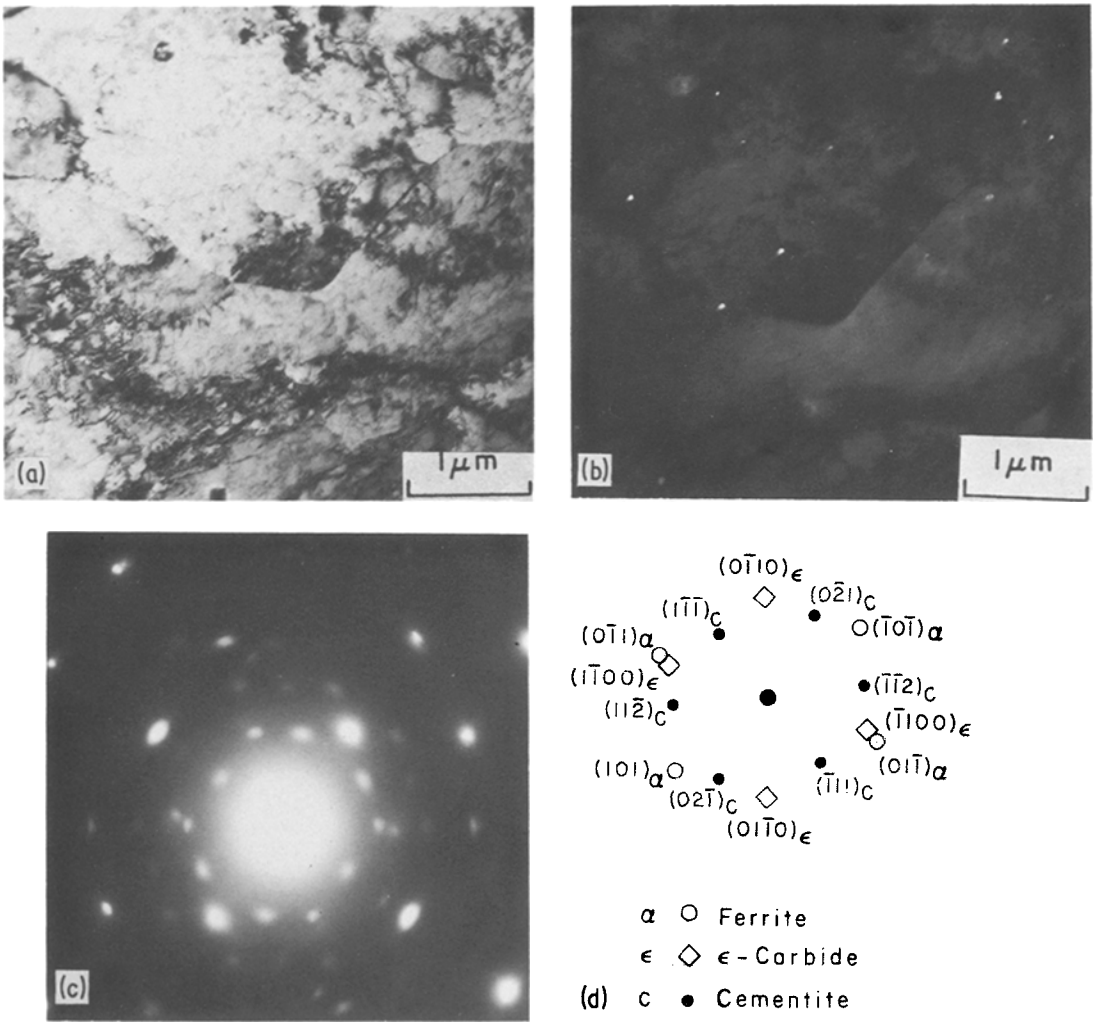

Figure 7 Transmission electron micrographs of laser-processed Fe–5% Cr alloy. (a) Bright-field; (b) dark-field, showing epsilon carbide using (1100) spot; (c) SAD pattern; (d) analysis of SAD.

4. Conclusions

A comparative study of the transformation behaviour of laser surface alloyed Fe–0.5% Cr, Fe–5% Ni and Fe–6% Cr–2% Ni alloys has been made. The principal results are:

1. Fe–5% Cr alloy undergoes a massive transformation to ferrite while Fe–5% Ni and Fe–6% Cr–2% Ni alloys undergo a transformation to a structure consisting of ferrite and martensite;

2. all three alloys exhibited both cementite and epsilon carbide;

3. solidification structures were observed only in Fe–5% Ni and Fe–6% Cr–2% Ni alloys.

Acknowledgement

This work was supported by the US Army Research Office.

References

1. A. GILBERT and W. S. OWEN, *Acta Metall.* **10** (1962) 45.
2. W. S. OWEN, E. A. WILSON and T. BELL, "High Strength Materials", edited by V. F. Zackay (Wiley, New York, 1965) p. 167.
3. G. R. SPEICH and P. R. SWANN, *J. Iron Steel Inst.* **203** (1965) 480.
4. J. S. PASCOVER and S. V. RADCLIFFE, *Trans. TMS AIME* **242** (1968) 673.
5. T. BELL and W. S. OWEN, *ibid.* 239 (1967) 1940.
6. J. S. PASCOVER and S. V. RADCLIFFE, *Acta Metall.* **17** (1969) 321.
7. R. F. VYHNAL and S. V. RADCLIFFE, *ibid.* **15** (1967) 1475.
8. R. H. GOODENOW and R. F. HEHEMANN, *Trans. AIME* **233** (1965) 1777.
9. T. L. WILSON, J. K. JACKSON and R. E. MINER, *ibid.* **245** (1969) 2185.
10. W. D. SWANSON and J. G. PARR, *J. Iron Steel*

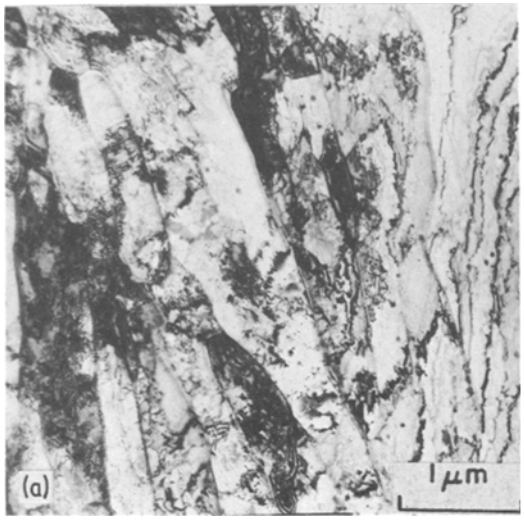

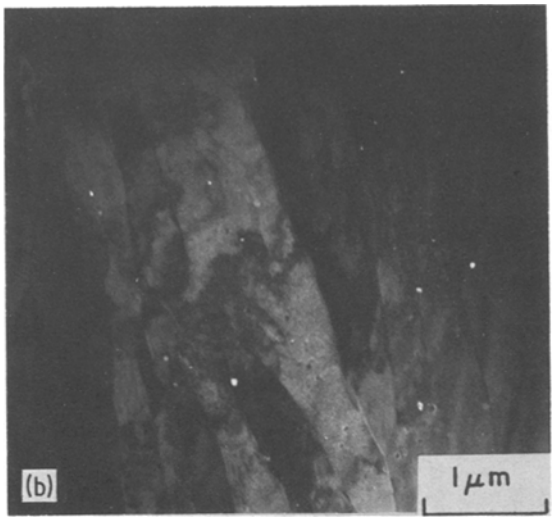

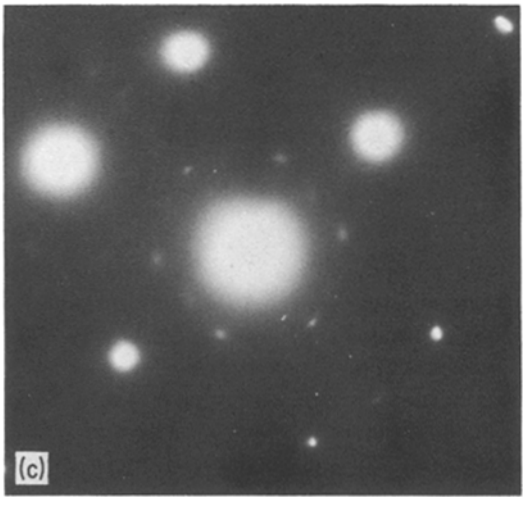

Figure 8 Transmission electron micrographs of laser-processed Fe–6% Cr–2% Ni alloy. (a) Bright-field; (b) dark-field showing M_3C using (021) spot; (c) SAD pattern.

Inst. **202** (1964) 104.
11. J. V. BEE and R. W. HONEYCOMBE, *Met. Trans.* **9A** (1978) 587.
12. W. E. BROWER, R. STRACHAN and M. C. FLEMINGS, *AFS cast Metals Res. J.* **12** (1970) 176.
13. W. F. SAVAGE, C. D. LUNDIN and A. H. ARONSON, *Welding J.* **44** (1965) 175-S.
14. T. B. MASSALSKI, *Acta Metall.* **6** (1958) 243.
15. G. R. SPEICH, "Metals Handbook", Vol. 8 (ASM, Metals Park, Ohio, 1973) p. 425.
16. H. E. CLINE and T. R. ANTHONY, *J. Appl. Phys.* **48** (1977) 3895.
17. J. W. WALLBRIDGE and J. G. PARR, *J. Iron Steel Inst.* **204** (1966) 119.
18. E. A. OWENS and Y. H. LIU, *ibid.* **163** (1949) 132.
19. J. W. PUGH and J. G. NISBET, *Trans. Amer. Inst. Min. Metall. Pet. Engg.* **188** (1950) 273.
20. C. S. ROBERTS, B. L. AVERBACH and M. COHEN, *Trans. ASM* **45** (1953) 576.
21. E. TEKIN, PhD thesis, Leeds University (1964).
22. A. R. COX, *Iron Steel* **12** (1968) 539.
23. W. C. LESLIE, *Acta Metall.* **9** (1961) 1004.
24. K. F. HALE and M. McLEAN, *J. Iron Steel Inst.* **201** (1963) 331.
25. M. G. H. WELLS and J. F. BUTLER, *Trans. ASM* **59** (1966) 427.

Received 11 May
and accepted 26 May 1982